

# Nuclear radius deduced from proton diffraction by a black nucleus

Akihisa Kohama,<sup>1</sup> Kei Iida,<sup>1</sup> and Kazuhiro Oyamatsu<sup>1,2,3</sup>

<sup>1</sup>*RIKEN (The Institute of Physical and Chemical Research),  
2-1 Hirosawa, Wako-shi, Saitama 351-0198, Japan*

<sup>2</sup>*Department of Media Theories and Production, Aichi Shukutoku University,  
Nagakute, Nagakute-cho, Aichi-gun, Aichi 480-1197, Japan*

<sup>3</sup>*Department of Physics, Nagoya University, Furo-cho, Chigusa-ku, Nagoya, Aichi 464-8602, Japan*

(Dated: October 23, 2018)

We find a new method to deduce nuclear radii from proton-nucleus elastic scattering data. In this method a nucleus is viewed as a “black” sphere. A diffraction pattern of protons by this sphere is equivalent to that of the Fraunhofer diffraction by a circular hole of the same radius embedded in a screen. We determine the black sphere radius in such a way as to reproduce the empirical value of the angle of the observed first diffraction peak. It is useful to identify this radius multiplied by  $\sqrt{3/5}$  with the root-mean-square matter radius of the target nucleus. For most of stable isotopes of masses heavier than 50, it agrees, within the error bars, with the values that were deduced in previous elaborate analyses from the data obtained at proton incident energies higher than  $\sim 800$  MeV.

PACS numbers: 21.10.Gv, 24.10.Ht, 25.40.Cm

Size of atomic nuclei, one of the most fundamental nuclear properties, remains to be determined precisely. Most popularly, the size is deduced from electron and proton elastic scattering off nuclei [1, 2, 3, 4, 5]. The charge radii are well determined due to our full understanding of the underlying electromagnetic interactions [5, 6, 7], while deduction of the matter radii from the proton-nucleus scattering data depends on the scattering theory, which is more or less approximate in the sense that the nucleon-nucleon interactions involved are not fully understood. During the past three decades there have been many efforts of deducing the matter density distributions, which are based on various scattering theories incorporating empirical nucleon-nucleon scattering amplitudes, such as Glauber theory [1, 3] and nonrelativistic and relativistic optical potential methods [8, 9, 10, 11]. A systematic analysis of the data for a large number of nuclides, however, is still missing. In this paper we propose a method to deduce the root-mean-square (rms) matter radii, which is powerful enough to allow us to perform such a systematic analysis. This method, in which we assume that the target nucleus is completely absorptive to the incident proton and hence acts like a “black” sphere, is far simpler than the conventional methods. This approximation was originally used by Placzek and Bethe [12] in describing the elastic scattering of fast neutrons.

The present method is useful for heavy stable nuclei for which the proton elastic scattering data are present, as we shall see. In the conventional framework to deduce the rms radius, one tries to reproduce empirical data for the differential cross section for scattering angles covering several diffraction maxima [1, 4, 13], whereas, in the present method, one has only to analyze the data around a maximum in the small angle regime. Remarkably, these two methods turn out to be similar in the deducibility of the radius.

Elastic scattering data for more neutron-rich unstable nuclei are expected to be provided by radioactive ion beam facilities, such as GSI and Radioactive Ion Beam Factory in RIKEN. In a possible scheme, a beam of unstable nuclei, such as Ni and Sn isotopes, created in heavy-ion collisions is incident on proton targets, and the protons scattered therefrom are detected, leading to the measurement of differential elastic cross section. We expect the present method to be effective at deducing the rms radius of unstable nuclei from such measurement.

We begin by regarding a target nucleus for proton elastic scattering as a black sphere of radius  $a$ . This picture holds when the target nucleus is completely absorptive to the incident proton. For high incident kinetic energy  $T_p$  above  $\sim 800$  MeV, the optical potential for this reaction is strongly absorptive. It can be essentially viewed as a superposition of the nucleon-nucleon scattering amplitude. Since the imaginary part of the amplitude is dominant over the real part in this energy range [14, 15], the black sphere picture is applicable to a first approximation. We note that the black sphere picture is fairly successful in describing the elastic scattering of low energy  $\alpha$  particles [4, 16]. It was also used for analyses of the scattering of intermediate-energy pions and low-energy antiprotons [4].

Since one can regard the proton beam as a plane wave of momentum  $p_{\text{Lab}} = \sqrt{(T_p + m_p)^2 - m_p^2}$  with the proton mass,  $m_p$ , the black sphere picture can be described in terms of wave optics. This picture reduces to a diffraction of the wave by a circular black disk of radius  $a$  if the corresponding wave optics is close to the limit of geometrical optics, i.e.,  $a/\lambda_{\text{Lab}} \gg 1$ , where  $\lambda_{\text{Lab}} = 2\pi/p_{\text{Lab}}$  is the wave length. We will later consider the ranges of  $T_p \gtrsim 800$  MeV and  $A \gtrsim 50$ , for which  $a/\lambda_{\text{Lab}} \gg 1$  is satisfied. According to Babinet’s principle, this diffraction is in turn equivalent to the Fraunhofer diffraction by a hole of the same shape as the disk embedded in a

screen [17]. The scattering amplitude for this diffraction in the center-of-mass (c.m.) frame of the proton and the nucleus reads

$$f(\mathbf{q}) = ipaJ_1(qa)/q, \quad (1)$$

where  $\mathbf{q}$  is the momentum transfer,  $\mathbf{p}$  is the proton momentum in the c.m. frame, and  $J_n$  is the  $n$ -th order Bessel function. We then obtain the differential cross section as  $d\sigma/d\Omega = |f(\mathbf{q})|^2$ . We remark that Eq. (1) can be obtained from the absorptive limit of the Glauber theory in which the phase shift function is approximated by  $\exp[i\chi(b)] = \theta(b-a)$ , where  $\mathbf{b}$  is the impact parameter perpendicular to  $\mathbf{p}$ , and  $f(\mathbf{q})$  is given by [18]

$$f(\mathbf{q}) = ip \int_0^\infty b db J_0(qa) \{1 - \exp[i\chi(b)]\}. \quad (2)$$

We assume that the density distribution of the black sphere is uniform. Then it is natural to introduce an rms black sphere radius,  $r_{\text{BS}}$ , as

$$r_{\text{BS}} \equiv \sqrt{3/5}a. \quad (3)$$

In this stage, we determine  $a$  in such a way that the c.m. scattering angle  $[\theta_{\text{c.m.}} \equiv 2 \sin^{-1}(q/2p)]$  of the first maximum for the Fraunhofer diffraction agrees with that measured by proton-nucleus elastic scattering,  $\theta_M$ . (Here we define the zeroth peak as that whose angle corresponds to  $\theta_{\text{c.m.}} = 0$ .) We remark that the diffraction patterns for  $\theta_{\text{c.m.}} \gg \theta_M$  are distorted by multiple scattering effects [1], which are beyond the scope of the black sphere picture. The radius,  $a$ , and the angle,  $\theta_M$ , are then related by

$$2pa \sin(\theta_M/2) = 5.1356 \dots \quad (4)$$

Combining this with Eq. (3), we may thus write

$$r_{\text{BS}} = \frac{3.9780 \dots}{2p \sin(\theta_M/2)}. \quad (5)$$

It is this formula that we use in the followings. As we shall see for heavy stable nuclei, the values of  $r_{\text{BS}}$  that can be determined from Eq. (5) agree well with the values of the rms matter radius,  $r_m$ , deduced from elaborate scattering theories in previous works. For the estimate of  $r_{\text{BS}}$  from the data for  $T_p \gtrsim 800$  MeV and  $A \gtrsim 50$ , one can use the approximate expression,

$$r_{\text{BS}} \simeq 4.50 \left( \frac{1 \text{ GeV}}{p_{\text{Lab}}} \right) \left( \frac{10 \text{ deg}}{\theta_M} \right) \text{ fm}. \quad (6)$$

For  $^{58}\text{Ni}$  and  $T_p = 1047$  MeV, the diffraction pattern is calculated from Eq. (1) by setting the first peak angle at  $\theta_M$ . The result is shown in Fig. 1 together with the experimental data [19]. The heights of the diffraction maxima and minima thus calculated deviate from the empirical values, because the black sphere picture does not allow for the surface diffuseness. That is why we

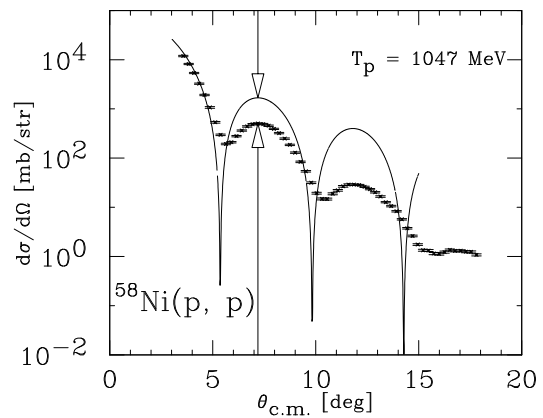


FIG. 1: Differential cross section calculated from the Fraunhofer diffraction formula, Eq. (1), for  $p$ - $^{58}\text{Ni}$  elastic scattering ( $T_p = 1047$  MeV). The experimental data (crosses) are taken from Ref. [19]. The arrows represent the first diffraction maximum, at which we fit the calculated peak angle to the empirical value.

pay attention to the scattering angles of the diffraction maxima and minima. The relation of these scattering angles to nuclear sizes has been discussed by Amado *et al.* [20] in the Glauber theory. The diffraction maxima are more advantageous to our study than the diffraction minima. This is partly because statistical uncertainties in the yield count are much smaller near the maxima than near the minima and partly because theoretical prediction of the minima is rather sensitive to spin-orbit and Coulomb interactions between nucleons [1]. We remark that the behavior around the first diffraction peak can be well reproduced by incorporating nucleon distributions similar to the rectangular distribution assumed here into the Glauber theory (see Fig. 1 in Ref. [21]).

It is important to note experimental uncertainty in the scattering angle and in the proton incident energy since this gives rise to the uncertainty in the estimate of  $r_{\text{BS}}$ , together with systematic errors that are dependent on the way of determining the peak position. The uncertainty in the measured angle, which is due mainly to the absolute angle calibration, is typically of order or smaller than  $\pm 0.03$  deg [22] for existing data for proton elastic scattering off stable nuclei, while the uncertainty in the measured proton incident energy is typically a few MeV [22].

In this work we focus on the proton elastic scattering data for  $A \gtrsim 50$ ,  $T_p \gtrsim 800$  MeV, and  $\theta_{\text{c.m.}} \gtrsim 5$  deg. We first display the Ni results for  $r_{\text{BS}}$ , which are obtained from the experimental values of  $\theta_M$  using Eq. (5). We have used the data for  $T_p = 796$  MeV [23, 24, 25],  $T_p = 1040$  MeV [26], and  $T_p = 1047$  MeV [19]. In collecting the data, we have made access to Experimental Nuclear Reaction Data File (EXFOR [CSISRS]) [27]. In Fig. 2, the values of  $r_{\text{BS}}$  derived from these data are plotted together with the deduced values of  $r_m$ . When the values of  $r_m$  are not explicitly given in the literatures, we obtain them from  $r_m^2 = (Z/A)r_p^2 + [(A-Z)/A]r_n^2$ , where  $Z$  is

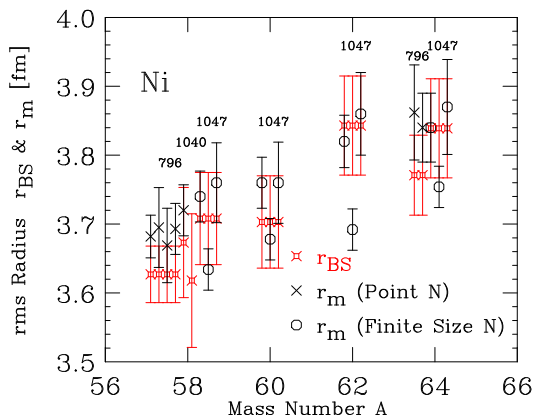


FIG. 2: (Color) The values of  $r_{BS}$  (squares) for Ni isotopes. For the error bars, see text. The values of  $T_p$  (in MeV) are specified above these error bars. For comparison we also plot the results for  $r_m$  derived in the following references: For  $A = 58$ , in Refs. [14, 22, 23, 24, 25] ( $T_p = 796$  MeV) and in Refs. [19, 28, 29] ( $T_p = 1047$  MeV); for  $A = 60$  and  $62$ , in Refs. [19, 28, 29]; for  $A = 64$ , in Refs. [14, 25] ( $T_p = 796$  MeV) and in Refs. [19, 28, 29] ( $T_p = 1047$  MeV). The crosses ( $\times$ ) denote the rms matter radii of the point nucleon distributions, and the circles ( $\circ$ ) denote those folded with the nucleon form factor. Only  $r_{BS}$  is plotted for  $A = 58$  and  $T_p = 1040$  MeV, because no  $r_m$  is available for this case.

the charge number, and  $r_p$  and  $r_n$  are the rms radii of the proton and neutron distributions. The values of  $\theta_M$  are determined from the scattering angle that gives the maximum value of the cross section among discrete data near the first diffraction maximum. The error bars of  $r_{BS}$  in the plot, which are of order or even greater than  $\pm 0.05$  fm, are determined from the half width between the neighboring angles measured. Uncertainties of  $r_{BS}$  associated with the absolute angle calibration and the measurement of  $T_p$ , which are smaller than  $\pm 0.03$  fm and  $\pm 0.02$  fm, respectively, are not taken into account. When the error of  $r_m$  is not available, we evaluate it from the errors of  $r_n$  and  $r_p$  given in the literatures.

We find from Fig. 2 that for all the isotopes, the values of  $r_{BS}$  agree with those of  $r_m$  within the error bars except for an only case. This result is remarkable since there is no fitting parameter other than  $a$  in the black sphere picture in contrast to the past elaborate analyses. We note that it is premature to ask whether we have to regard  $r_{BS}$  as an rms radius of the point nucleon distribution or as an rms matter radius folded with the nucleon form factor. In fact, the present estimate of  $r_{BS}$  contains errors larger than the difference between these two radii, which is typically  $\sim 0.07$  fm.

We next show the relations between  $r_{BS}$  and  $r_m$  in Fig. 3, which are constructed from systematic data for various stable nuclides of mass number larger than 50. In deriving  $r_{BS}$  we have used the data for  $^{54}\text{Fe}$  ( $T_p = 796$  MeV) [25],  $^{90}\text{Zr}$  ( $T_p = 800$  MeV) [35],  $^{90}\text{Zr}$  ( $T_p = 1000$  MeV) [36],  $^{116,124}\text{Sn}$  ( $T_p = 800$  MeV) [32], and  $^{208}\text{Pb}$  ( $T_p = 800$  MeV) [23, 35],  $^{208}\text{Pb}$  ( $T_p = 1000$  MeV) [36],

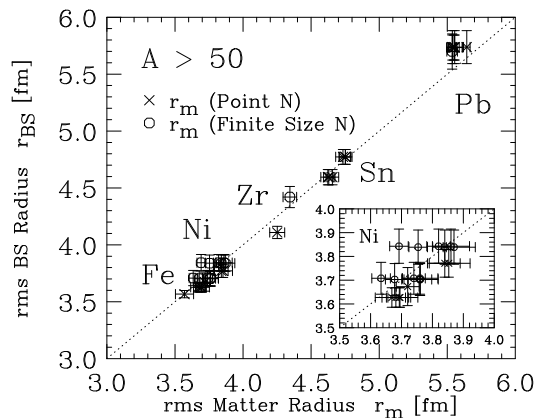


FIG. 3:  $r_{BS}$  vs.  $r_m$  for stable nuclei of masses above 50. For Ni isotopes the values of  $r_m$  are taken from the same references as cited in Fig. 2; for  $^{54}\text{Fe}$ , from Ref. [25]; for  $^{90}\text{Zr}$ , from Refs. [22, 30, 31]; for  $^{116,124}\text{Sn}$ , from Refs. [14, 22, 32]; for  $^{208}\text{Pb}$ , from Refs. [14, 22, 23, 30, 31, 33, 34]. The definition of the crosses ( $\times$ ) and the circles ( $\circ$ ) is the same as in Fig. 2. The dotted line represents  $r_{BS} = r_m$ . Inset:  $r_{BS}$  vs.  $r_m$  for Ni isotopes.

We do not include the data of  $^{208}\text{Pb}$  ( $T_p = 1040$  MeV) [26] in this analysis, because the first peak position is not clear. The data for Ni isotopes are the same as used in Fig. 2. We can see that the values of  $r_{BS}$  and  $r_m$  including the error bars are mostly on the line of  $r_{BS} = r_m$ . We thus find that  $r_{BS}$  provides a good measure of the rms matter radius. If elastic scattering data are obtained in a much finer manner, the main uncertainty in  $r_{BS}$  would arise from the absolute angle calibration and possibly the measurement of  $T_p$ . In any case one could nicely determine the isotope dependence of  $r_{BS}$  if the relative peak angles between isotopes are accurately measured for the same proton beam.

For nuclides for which elastic scattering data are available but no  $r_m$ , we list the values of  $r_{BS}$  for reference. For  $^{90}\text{Zr}$  ( $T_p = 800$  MeV) [37], we obtain  $r_{BS} = 4.22 \pm 0.10$  fm; for  $^{90}\text{Zr}$  ( $T_p = 800$  MeV) [38],  $r_{BS} = 4.21 \pm 0.11$  fm; for  $^{92}\text{Zr}$  ( $T_p = 800$  MeV) [38],  $r_{BS} = 4.21 \pm 0.07$  fm; for  $^{120}\text{Sn}$  ( $T_p = 800$  MeV) [37],  $r_{BS} = 4.62 \pm 0.10$  fm; for  $^{144}\text{Sm}$  ( $T_p = 800$  MeV) [37],  $r_{BS} = 4.92 \pm 0.27$  fm; for  $^{154}\text{Sm}$  ( $T_p = 800$  MeV) [39],  $r_{BS} = 5.24 \pm 0.09$  fm; for  $^{176}\text{Yb}$  ( $T_p = 800$  MeV) [39],  $r_{BS} = 5.47 \pm 0.10$  fm; for  $^{208}\text{Pb}$  ( $T_p = 800$  MeV) [37],  $r_{BS} = 5.54 \pm 0.29$  fm. Among these nuclei,  $^{154}\text{Sm}$  and  $^{176}\text{Yb}$  are deformed in the ground state. Since cross sections are generally measured for proton elastic scattering from randomly oriented nuclei, the disk radius,  $a$ , obtained from the data lies between the lengths of the semimajor and semiminor axes of the deformed nuclei. As long as the degree of deformation is small, therefore,  $r_{BS}$  is expected to give a good measure of the rms matter radii of the deformed nuclei.

In summary we have performed a systematic analysis, based on the Fraunhofer diffraction off a black disk, of the existing data for proton elastic scattering off stable nuclei with masses larger than 50 at proton incident

energies above  $\sim 800$  MeV. This analysis allows us to make systematic estimates of the rms matter radii. The present method works even for the data in a range of  $\mathbf{q}$  covering only the first diffraction maximum. Such cases would occur for neutron-rich unstable nuclei. By combining the present result with a comprehensive table for the rms charge radii [6, 7], we can estimate neutron skin thickness for various nuclides on equal footing. This is an important step towards understanding of the isospin-dependent bulk and surface properties of nuclear matter [40].

In the near future, an experiment that provides differential cross sections of proton elastic scattering off Ni unstable isotopes will be performed in GSI. In this experiment the projectile will be a radioactive ion beam having energy per nucleon of about 400 MeV, and the scattering angles to be measured will contain the first diffraction maximum. In applying the present prescription to estimate the rms matter radius to such measurements, its validity, which has been confirmed here for proton incident energies above  $\sim 800$  MeV, needs to be examined at relatively low bombarding energies. Investigation of how  $r_{\text{BS}}$  depends on the bombarding energy is now in

progress [41]. Once the values of  $r_{\text{BS}}$  are accumulated for various nuclides including neutron-rich heavy nuclei, it is expected that the density dependence of the symmetry energy near normal nuclear density will be clarified [42]. This expectation is also suggested by the work [21] that pointed out the relation of  $\theta_M$  with the density dependence of the symmetry energy. We note, however, that the estimate of  $r_{\text{BS}}$  depends strongly on how sharp the energy distribution of a radioactive ion beam will be.

In order to deduce the surface diffuseness in addition to the rms radius, one has to reproduce the overall behavior of the elastic scattering differential cross sections, as shown in Refs. [1, 4, 13]. The tails of the distributions, which are hard to deduce from the differential cross sections, might affect the prediction of reaction cross sections [43]. If reaction cross sections are measured for various heavy nuclides, the “halo” structure of unstable nuclei and the tails for stable nuclei will become clearer.

We acknowledge K. Yazaki for his invaluable suggestions and comments. This work is supported in part by RIKEN Special Postdoctoral Researchers Grant No. A11-52040.

- 
- [1] G.D. Alkhozov, S.L. Belostotsky, and A.A. Vorobyov, *Phys. Rep.* **42**, 89 (1978).
- [2] A. Chaumeaux, V. Layly, and R. Schaeffer, *Ann. Phys.* **116**, 247 (1978).
- [3] G.J. Igo, *Rev. Mod. Phys.* **50**, 523 (1978).
- [4] C.J. Batty, E. Friedman, H.J. Gils, and H. Rebel, *Adv. Nucl. Phys.* **19**, 1 (1989).
- [5] B. Frois, C.N. Papanicolas, and S.E. Williamson, *Modern Topics in Electron Scattering*, edited by B. Frois and I. Sick (World Scientific, 1991), p. 352.
- [6] H. de Vries, W. de Jager, and C. de Vries, *At. Data Nucl. Data Tables* **36**, 495 (1987).
- [7] G. Fricke *et al.*, *At. Data Nucl. Data Tables* **60**, 177 (1995).
- [8] L. Ray, G. Hoffmann, and W.R. Coker, *Phys. Rep.* **212**, 223 (1992).
- [9] E.D. Cooper, S. Hama, B.C. Clark, and R.L. Mercer, *Phys. Rev. C* **47**, 297 (1993).
- [10] B.C. Clark, L.J. Kerr, and S. Hama, *Phys. Rev. C* **67**, 054605 (2003).
- [11] H. Sakaguchi *et al.*, *Phys. Rev. C* **57**, 1749 (1998).
- [12] G. Placzek and H.A. Bethe, *Phys. Rev.* **57**, 1075 (1940).
- [13] A. Kohama, R. Seki, A. Arima, and S. Yamaji, *J. Phys. Soc. Japan* **72**, 2766 (2003).
- [14] L. Ray, *Phys. Rev. C* **19**, 1855 (1979).
- [15] L. Ray, *Phys. Rev. C* **20**, 1857 (1979).
- [16] B. Fernandez and J.S. Blair, *Phys. Rev. C* **1**, 523 (1970).
- [17] L.D. Landau and E.M. Lifshitz, *Classical Theory of Fields* (Pergamon, Oxford, 1975).
- [18] R.J. Glauber, *Lectures in Theoretical Physics, Vol. I*, edited by W.E. Brittin and D.G. Dunham (Interscience, New York, 1959), p. 315.
- [19] R.M. Lombard, G.D. Alkhozov, and O.A. Domchenkov, *Nucl. Phys.* **A360**, 233 (1981).
- [20] R.D. Amado, J.P. Dedonder, and F. Lenz, *Phys. Rev. C* **21**, 647 (1980).
- [21] K. Iida, K. Oyamatsu, and B. Abu-Ibrahim, *Phys. Lett. B* **576**, 273 (2003).
- [22] L. Ray, W. Rory Coker, and G.W. Hoffmann, *Phys. Rev. C* **18**, 2641 (1978).
- [23] G.S. Blanpied *et al.*, *Phys. Rev. Lett.* **39**, 1447 (1977); Erratum *ibid.* **40**, 420 (1978).
- [24] G.S. Kyle *et al.*, *Phys. Lett.* **91B**, 353 (1980).
- [25] G.W. Hoffmann *et al.*, *Phys. Lett.* **79B**, 376 (1978).
- [26] R. Bertini *et al.*, *Phys. Lett.* **45B**, 119 (1973).
- [27] Nuclear Data Centers Network, *EXFOR Systems Manual: Nuclear Reaction Data Exchange Format*, Report BNL-NCS-63330 (1996), compiled and edited by V. McLane, National Nuclear Data Center, Brookhaven National Laboratory, U.S.A.
- [28] G.D. Alkhozov *et al.*, *Phys. Lett.* **67B**, 402 (1977).
- [29] A. Chaumeaux, V. Layly, and R. Schaeffer, *Phys. Lett.* **72B**, 33 (1977).
- [30] L. Ray *et al.*, *Phys. Rev. C* **18**, 1756 (1978).
- [31] G.D. Alkhozov *et al.*, *Nucl. Phys.* **A381**, 430 (1982).
- [32] G.W. Hoffmann *et al.*, *Phys. Lett.* **76B**, 383 (1978).
- [33] G.S. Blanpied *et al.*, *Phys. Rev. C* **18**, 1436 (1978).
- [34] G.W. Hoffmann *et al.*, *Phys. Rev. C* **21**, 1488 (1980).
- [35] G.W. Hoffmann *et al.*, *Phys. Rev. Lett.* **40**, 1256 (1978).
- [36] G.D. Alkhozov *et al.*, Preprint LNPI-531, Leningrad (1979).
- [37] M.M. Gazzaly *et al.*, *Phys. Rev. C* **25**, 408 (1982).
- [38] F. Todd Baker *et al.*, *Nucl. Phys.* **A393**, 283 (1983).
- [39] M.L. Barlett *et al.*, *Phys. Rev. C* **22**, 1168 (1980).
- [40] K. Iida and K. Oyamatsu, *Phys. Rev. C* **69**, 037301 (2004).
- [41] A. Kohama, K. Iida, and K. Oyamatsu (unpublished).
- [42] K. Oyamatsu and K. Iida, *Prog. Theor. Phys.* **109**, 631

- (2003).
- [43] A. Ozawa, T. Suzuki, and I. Tanihata, Nucl. Phys. **A693**, 32 (2001).